

## SEDS Deployer Design and Flight Performance

Joseph A. Carroll\*  
Tether Applications  
Chula Vista, CA 91913  
(619) 421-2100, -2111 fax

### Abstract

The Small Expendable Deployment System (SEDS) was conceived as a complement to the Tethered Satellite System deployer for use when tether retrieval is not required. This paper reviews the history, design, and capabilities of SEDS, and discusses its flight performance, based on data collected during the successful SEDS-1 flight experiment.

### Introduction: SEDS Project History

In 1983, the author developed the concept of a small expendable deployment system (SEDS) and wrote an SBIR proposal to develop it at Energy Science Laboratories (ESL). This led to SBIR Phase I and II contracts with NASA Marshall Space Flight Center (MSFC)<sup>1</sup>. That work further stimulated NASA interest in SEDS and led to two follow-on contracts: to define the SEDS-1 flight experiment<sup>2</sup> and to design and fabricate flight hardware for SEDS-1. In parallel with this work, MSFC personnel developed a Bight computer to control SEDS and collect flight data. In 1989, the author split off from ESL to form Tether Applications, which has assisted MSFC in integrating and flying SEDS-1.

NASA was initially interested in shuttle-based SEDS experiments, but the focus shifted to expendable vehicles after the Challenger accident. Delta/GPS launches seemed suitable because they left the Delta second stage in suitable orbits and had significant payload margin. The Air Force developed a policy encouraging use of this payload margin for government-sponsored payloads on a non-interference, marginal-cost-reimbursement basis<sup>3</sup>. This led to a NASA commitment to fly SEDS-1, SEDS-2, and the PMG (Plasma Motor Generator) on Delta/GPS missions. All three mount in the same place on the Delta, with the same interface. SEDS-1 flew on March 29, 1993, and the PMG on June 24, 1993. Both were successful. SEDS-2 is scheduled to fly in March 1994. Other missions await determination of Delta payload margins, launch schedules, and integration costs.

\* Proprietor, Tether Applications; AIAA member.  
Copyright © 1993 by Joseph A. Carroll. Published by the AIAA with permission.

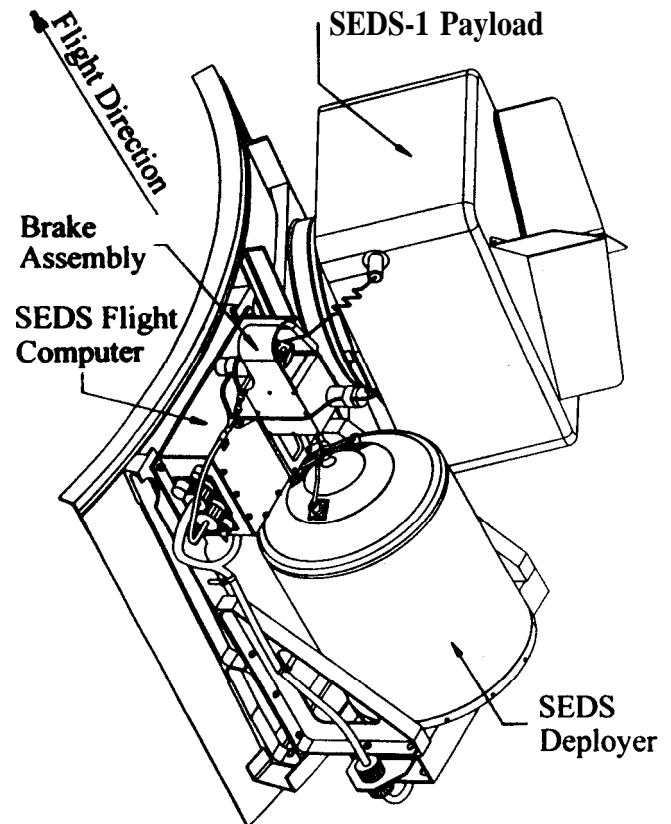


Figure 1. SEDS Deployer and Payload Mounted on Delta

### Evolution of SEDS Design

Figure 1 shows the SEDS flight deployer mounted on the Delta. Figure 2 shows the brake in cross-section, and Figure 4 the deployer. The best way to explain many key features is to describe the evolution that led to them.

SEDS was conceived as a complement to the NASA TSS (Tethered Satellite System), for cases in which tether retrieval is not needed. Simulations showed that deployment at low tension had two significant benefits in payload boosting or deboosting: it allowed use of a simpler brake, and it induced a wide libration that nearly doubled the deltaV provided by a given length of tether.

The initial SEDS design had a fixed “criss-cross” winding inside a shuttle GAS canister. The tether paid off one end of the winding, with spring-loaded flaps pressing lightly against the winding to guarantee orderly payout. During deployment this caused large tension variations, but the absolute tension was low enough that this was not considered a problem. Simulations showed that ramping tension up near the end would save several times the deployer’s weight in RCS propellant, so we substituted gas-bags and a gas supply for the spring-loaded flaps.

Deployment tests in air and in vacuum showed that the tension had a fixed component and a velocity-squared component, with the  $V^2$  term dominant at deployment velocities above roughly 5 m/s. This sensitivity seemed useful because of its potential for damping undesired deployment dynamics without any need for measurement or active control. Simulations showed that this passive damping would be far more effective if it could be amplified near the end of deployment (i.e., if the brake were multiplicative rather than additive). This led us to consider “tortuous-path” brakes, which impose a friction that scales with the upstream tension. We selected the “barberpole” design shown in Figure 2 because it is easy to heat sink and has a nearly uniform exponential sensitivity over a very wide range. Braking is applied by a small stepper motor which drives a worm gear at the base of the brake post. A tether guide in the worm gear wraps tether spiral-fashion around the post. Each wrap around the post roughly triples the outboard tension.

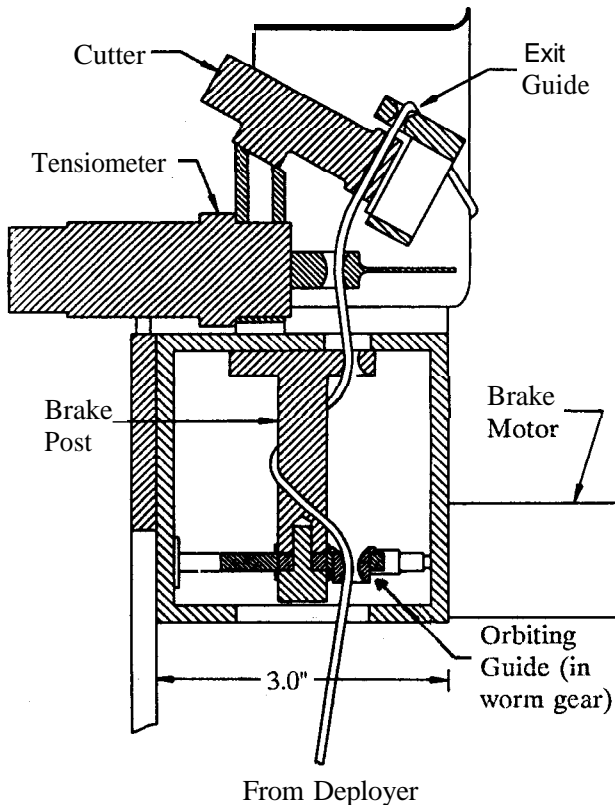


Figure 2. Cross-section of SEDS “Barberpole” Brake

The barberpole brake allowed us to eliminate squeegee flaps and bags, but required another way to hold the winding in place during handling and launch vibrations. We used a thread tie-down at each end of the winding, plus a third tie-down to adjust the length outside the deployer. The tie-downs reliably hold the package in place during launch vibrations, but after payload ejection they break at tether tensions of 15-30 newtons.

Deployment, tests done without active braking showed that the  $V^2$  tension term increased as the tether unwound. Thus a small core maximizes passive braking at the end of deployment. Removing the squeegee flaps and bags reduced but did not eliminate high-frequency tension variations. We found a way to radically reduce them late in deployment, when tension is highest. We put small flanges on the core and wound the innermost part of the winding parallel fashion in slightly conical layers. The parallel pattern reduced the axial cycle frequency by a factor of 60, and the proper cone angle made diameter effects cancel out axial effects. Residual tension variations with axial position are small, as will be seen from the flight data. Figure 3 shows the effect on high-frequency variations. It shows 8 seconds worth of 62 Hz tension data from a July 1992 deployment test, at the time the winding changed from criss-cross to conical.

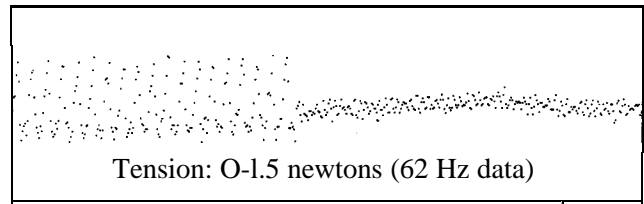


Figure 3. Tension due to Criss-cross and Cone Windings

## Other SEDS Design Features

Deployed length and deployment rate are determined by noting the time at which each turn deploys. The top end of the core holds infrared emitting diodes that point at phototransistors mounted on the top of the canister. As each turn unwinds, it shadows one phototransistor, then the other. Set-reset logic distinguishes turn counts from transverse tether oscillations, which typically add about 1% spurious counts on each channel. Other logic detects a channel failure and switches to counting turns on the other channel. The turn-counter was error-free on SEDS-1: all 46,216 turns wound onto the package were deployed and counted. Inspection of the time intervals indicates that all counts were physically meaningful.

The SEDS-1 brake law was based on turns unwound; the SEDS-2 brake law includes an approximate computation of length. Post-flight data analysis uses a computer record of the wound length at each turn, and includes compensation for tension and temperature differences between winding and deployment conditions.

The sensor holder in the top of the core also contains a reflective photo-pair that detects when the last 5% of the tether begins to deploy. This is used as the brake enable sensor if the turn-counter fails. The sensor holder also contains a thermister for core temperature measurement.

A side view of the deployer is shown below in Figure 4. The deployer bolts to a shelf mounted on the side of the Delta. It is held in place by four 1/4-28 bolts in a 2.25" bolt circle, plus (on SEDS-1) four 10-32 bolts near the rim. The baseplate can be modified for other patterns.

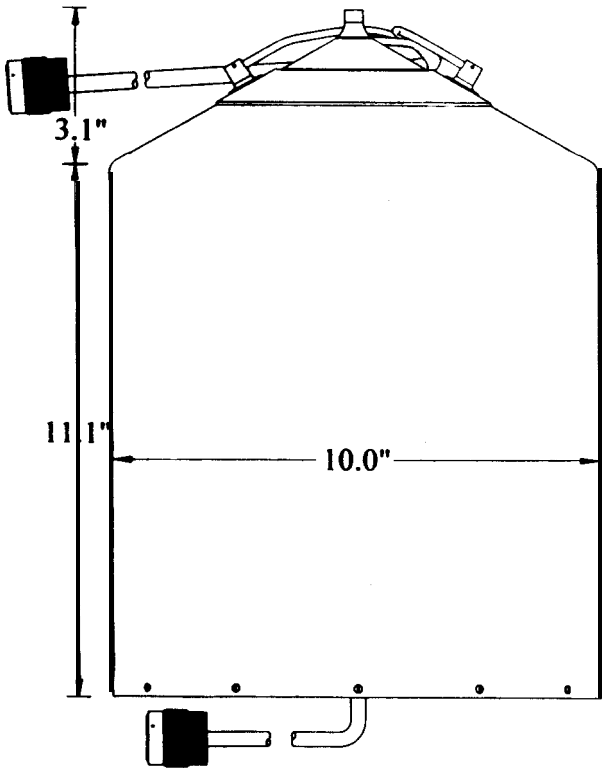


Figure 4. Side View of SEDS Deployer with Cabling

On SEDS-1, the computer started the brake motor after 41,026 turns had deployed (95% of the tether length). The brake rate was fixed at 1 wrap/minute, and did not use feedback to compensate for the faster-than-nominal deployment. This plus a friction coefficient slightly lower than expected decreased braking effectiveness. On SEDS-2, braking will begin much earlier, and feedback will be used to ensure the desired deployment rates.

The brake can apply loads up to the full breaking strength of the baseline 0.75 mm tether (750+ newtons). Much of the frictional heating goes into the tether itself rather than the brake. This gives the SEDS brake a total heat-dissipation capacity > 100 kJ, 14 times that needed for SEDS-1 and 5 times that needed for SEDS-2, without reaching a temperature that can damage the tether. Much higher capacities are possible by modifying a few brake components, or by wrapping the tether once or twice around a fixed heat sink outboard of the brake.

Instead of modifying the brake for very heavy payloads, an alternative is to deploy at low tension, closer to the horizontal. This greatly reduces brake loads and provides slightly larger delta Vs, at the cost of modest increases in deployment time and micrometeoroid risk.

In addition to the brake proper, the brake assembly also includes a running-line tensiometer, which uses an LVDT load cell that measures small displacements of a sprung tether guide. Interchangeable load cells with different spring rates allow a selection of full-scale tensions from 0.15 to 150 newtons, all with 1 mm full-scale travel. SEDS-1 and SEDS-2 both use a 7.5 newton range.

The sprung tensiometer guide vibrates significantly during deployment, so readings are taken at 500 Hz and digitally averaged. A code is stored with the average to indicate whether the digitized data includes out-of-range readings (0 or 255). Twice during deployment, 16 seconds worth of raw data are also recorded.

Above the tensiometer is a redundant pyrotechnic bolt cutter that has been qualified for TSS use on the shuttle. Mounted on the cutter is a tether exit guide. Friction around that guide increases outboard tension by 17-20% per radian of tether bend around the guide, compared to the tension measured by the LVDT.

The SEDS flight computer is an 8-bit computer based on the NSC800 microprocessor. It was designed by Chris Rupp of MSFC for use with the SEDS deployer, and was built at MSFC. The same type of computer was used to collect data on the SEDS-1 deployed payload. The computer has a multiplexed 8-bit A/D, 128K or 512K of mass RAM, and interface circuitry for the turn-counter, tensiometer, tether cutter, and telemetry output to the Delta. The computer collects the following data:

1. Time at which each turn of tether deploys ( $\pm 1$  ms)
2. Time brake-enabling sensor triggers (5% left)
3. Tension (500 Hz, summed down to 1 Hz)
4. Temperatures (0.1 Hz): core, can, brake, computer

### The SEDS Tether

The SEDS deployer holds up to 7.5 kg of Spectra tether or the same volume of other materials. The tether is pre-twisted during winding so it will pay off the spool without residual twist. In cases where controlled payload spin is desired, this can be changed. The crisscross part of the winding includes four different patterns (4, 5, 6, and 7 turns per axial cycle) for package stability.

The SEDS-1 tether was braided from Spectra 1000, a highly oriented polyethylene fiber made by Allied Fibers. It has the highest strength-to-weight ratio and best impact resistance of any commercially available fiber.

Spectra also has low friction, low abrasion sensitivity, low dust generation, and better UV resistance than Kevlar. Spectra has limited heat resistance. It will fail if exposed to steady-state aeroheating at altitudes near 130 km. (On SEDS-1, the tether probably remained attached to the payload down to about 110 km due to a rapid descent.) A Teflon overbraid is needed if atomic oxygen exposure exceeds roughly an hour at 150 km or a week at 300 km.

We have recently learned that small amounts of coconut oil are used as a "spinning aid" in producing and braiding Spectra. Deployment tests show that increased amounts of oil correlate with unacceptably high deployment tensions and with an increased tension variation with temperature. We are testing supercritical CO<sub>2</sub> extraction to remove this oil. This should reduce outgassing and may make SEDS useful in a wider range of applications.

The SEDS-1 tether was 20 km long and 0.75 mm in diameter. (There was room for another 3 km of tether in the deployer, but 20 km was sufficient to de-orbit payloads from Delta orbits having perigees up to 280 km.) The 0.75 mm diameter was large enough to limit micrometeoroid risks to about 0.1% during a one-orbit experiment. This diameter is also strong enough to allow use with full Delta primary payloads, since the 900 kg mass of the empty Delta 2<sup>nd</sup> stage limits the loads that can be imposed on the tether. Hence SEDS-1 was a test of an operationally useful system, not a scale model.

SEDS-1 tether fabrication involved braiding 8 strands of fibers into a hollow braid. After inspection, several such segments were spliced together end-to-end to form a 20 km flight tether. Segments need not be identical. For example, the first meter of the SEDS-1 tether was a thick Kevlar braid. The part of the Kevlar exposed before deployment was covered by heat shrink. This provided better heat resistance during boost and 3<sup>rd</sup> stage firing. This section of tether was given a sinusoidal set when the heat shrink was cooled, to provide a weak spring to take up slack before deployment. The heat shrink may also increase passive damping of payload attitude oscillations.

Objects can be embedded in the tether during braiding. For example, the SEDS-1 tether had a 100 m length of solder embedded in the last part of the tether to deploy, as a test of passive braking. In addition, 3-meter lengths of solder were embedded 1.3, 1.7, and 2.1 km from the end. Each section caused a 1/4 second doubling of the tension while it deployed. This injected a tensile wave into the 18-19 km of deployed tether. As indicated in ref. 4, each wave was detected at the payload end about 2.6 seconds later. When the waves returned to the deployer, they appear to have been entirely absorbed by its low dynamic impedance. (This can be seen in the flight data shown in Figure 7.)

A dipole array was also embedded at the midpoint of the tether length. It used 10 m of nylon monofilament with 100 25-mm long aluminized sections at 100 mm intervals. Unfortunately, C-band radar tracking opportunities on SEDS-1 ended before the array deployed, so we obtained no flight data on the array. But such an array should have a C-band radar cross section  $> 10 \text{ m}^2$  at 7 discrete angles. Glint timing should allow tether cone angle estimation to better than 1°. Polarization of the return should provide complementary clock angle data. On future experiments we may put 30-cm lengths of 42 AWG wire in the braid to ensure visibility to UHF radar.

## Integration and Launch Operations

SEDS-1 experiment costs were dominated by integration-related activities, so integration and launch operations will be discussed briefly as a guide to understanding possible constraints on future SEDS experiments.

During Delta 2<sup>nd</sup> stage fabrication over a year before flight, structural and electrical modifications were made to the 2<sup>nd</sup> stage electronics bay for SEDS. Holes were drilled and special cable harnesses were built up and installed. SEDS hardware was sent to Pueblo, CO for a fit-check when the 2<sup>nd</sup> stage was nearly complete. Three months before launch, the SEDS computer was hooked up to the Delta during checkout in Florida. About 10 days before launch, SEDS hardware was installed on the Delta, checked out, and powered down. It remained in that state until the primary Delta mission was complete.

In parallel with this, tests, simulations, and analyses were done on the SEDS deployer and payload, and frequent meetings and telecons reviewed the status of interface and integration issues. To reduce these costs in the future, it may make sense to make SEDS experiments electrically autonomous, even though this requires reliable protection against premature payload ejection or radio transmission.

Launch occurred in a window set by the GPS satellite. Three launch scrubs delayed launch a total of 10 days: 2 for weather and 1 for Delta ground support hardware. After launch, the solid motors fell away in two groups, 1 and 2 minutes after liftoff. The 1<sup>st</sup> stage fell away a few minutes later, and then the fairing. Ten minutes after liftoff, the 2<sup>nd</sup> stage reached a 185x185 km parking orbit.

Near the first equator crossing, the 2<sup>nd</sup> stage raised its apogee to 740 km provide a small assist to the 3<sup>rd</sup> stage, which is undersized for GPS Block 2 satellites. It then spun up and released the 3<sup>rd</sup> stage, which boosted the GPS satellite into a transfer orbit. The GPS satellite circularized its orbit at apogee. A plume shield protected the short exposed length of tether and most of the other SEDS hardware from the stage exhaust.

After 3<sup>rd</sup> stage ignition, activity on the 2<sup>nd</sup> stage could no longer affect primary mission success. However one item remained: a propellant depletion burn to safe the stage. On SEDS-1, this was done after the SEDS experiment, but on SEDS-2, the depletion burn will be done first, to allow the experiment to be open-ended. Gold gas will be retained for attitude control during the experiment.

### SEDS-1 Mission Scenario and Performance

Shortly before the first apogee of the 185 x 740 km orbit, the Delta 2<sup>nd</sup> stage rolled until the SEDS payload faced earth. It then provided power to the SEDS computer, at 3720 seconds after launch. The SEDS computer took 0.7 second to initialize. (Experiment times below are based on this SEDS computer time.) A minute later, the Delta fired pyrotechnic cutters that severed the bolts holding the Marman clamp together. Four springs ejected the SEDS payload at 1.6 m/sec. Payload ejection broke the three tie-downs holding the tether inside the deployer. The resulting jerks induced a payload attitude rate of several deg/sec. This induced payload oscillations about the tether attachment point, which caused transverse tether oscillations and significant variations in deployment rate. These lasted for about 3000 seconds. The rate variations were not predicted before flight, but have since been reproduced in detailed simulations by John Glaese<sup>5</sup>

Figure 5, below, shows second-by-second length, rate, and tension data, plus the times of various events. Tension is shown on two scales with MI-scale values of 0.5 and 8 newtons, to make the data readable over a wide range. Various features shown on Figure 5 are discussed below. The period after 4300 seconds is shown on an expanded horizontal scale in Figure 6, and is discussed later.

The tension was non-zero before deployment. This was due to the weak heat-shrink "spring". Tie-down breakage induced 3 large but brief tension-spikes which are estimated to have had peak tensions of 15-40 newtons based on ground tests. After payload ejection, the Delta rolled until the SEDS deployer was on the bottom. The average tether tension was only 0.03-0.04 newtons, but this was enough to reduce the deployment rate from 1.6 to 0.75 m/sec within 20 minutes. The slight reduction shown in measured tension during the first 1000 seconds may be due to drift in the tensiometer electronics or it may be real, due to reduced V<sup>2</sup> effects and/or tension averaging through increasing periods of slackness. (The turn-count data indicate intervals between turns of up to 3 seconds.) After 1500 seconds, orbital dynamics effects became dominant and deployment sped up. This made slip-stick behavior less common and increased V<sup>2</sup> damping. The result is a rapid reduction in deployment rate scatter, starting near 2000 seconds.

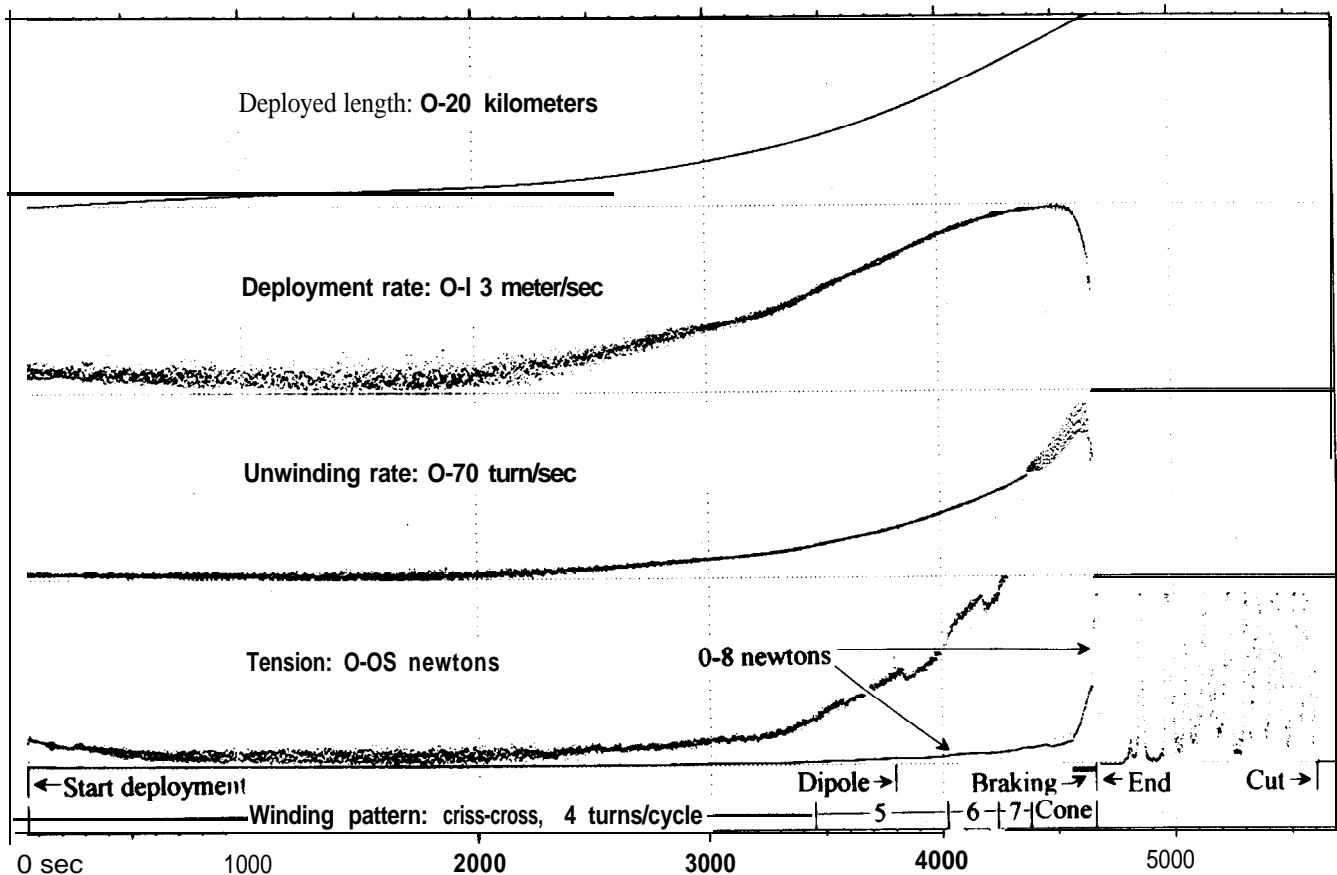


Figure 5. SEDS-1 Deployer Flight Data (1-sec averages)

Perigee occurred near 2900 seconds. Air drag on the tether near 185 km was enough to induce a bow in the tether. This caused the slight bulge in the deployment rate curve that is centered on 2900 seconds.

At 3450 seconds, the crisscross winding pattern changed from 4 turns per axial cycle to 5. This has little effect on deployment tension. At 3665 seconds, the Delta 2<sup>nd</sup> stage switched from pointing in the flight direction to a rate-damping mode, to limit cold-gas usage as tether tension increased. Shortly thereafter, the midpoint of the tether deployed with its embedded dipole array. Two adjacent 1-second tension values stand above the rest. This is compatible with lab test data which indicate a 25% tension increase during dipole deployment.

Shortly after dipole deployment, a very low frequency step-like oscillation began in the deployment tension, superimposed on an otherwise smooth tension ramp. This is most clearly visible near 4000 seconds, but can also be seen near 4500 seconds. The slight drops at the start of each new winding pattern were expected, but the rest of this variation needs further study.

The rest of the experiment is better studied on Figure 6, which shows the same data beginning at 4300 seconds, stretched horizontally by a factor of 4. The data are still one-second averages, but they are spread further apart.

The transition from criss-cross to conical parallel wind occurred at 4380 seconds. The deployment rate was slowly approaching its peak of 13 m/s. The conical layers of this final part of the winding caused a large triangular-waveform variation in turncount rate. The amplitude was small at first, since it involved partial layers. The amplitude grew and the frequency dropped as the conical layers reached further along the axis. Inspection of the data indicates the tension does not vary much on the lo-second time scale of a typical axial cycle. This indicates that the cone angle is about right. (By comparison, deployment tests with cylindrical rather than conical layers show a relative variation in tension that is comparable to that shown here in the unwinding rate.)

By 4500 seconds after ejection, tension had increased passively by a factor of 20, enough to overcome the increasing orbital dynamics effects and prevent further acceleration of deployment. The three short lengths of solder embedded in the tether deployed at 30-second intervals, injecting tensile waves into the tether which were damped when they returned to the deployer.

Figure 7 shows 16 seconds of high-rate tension data, starting just before deployment of the 1<sup>st</sup> solder segment. The 90 Hz data shown eliminates the free resonance of the tensiometer by averaging groups of 5.55 samples, with fractional weighting used for values at group boundaries.

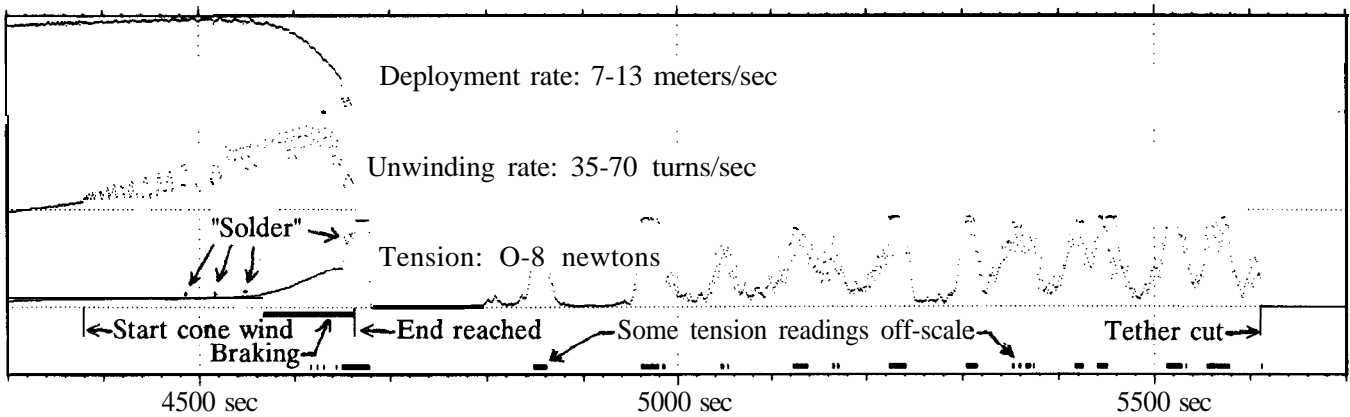


Figure 6. SEDS-1 Flight Data (4300 to 5700 seconds)

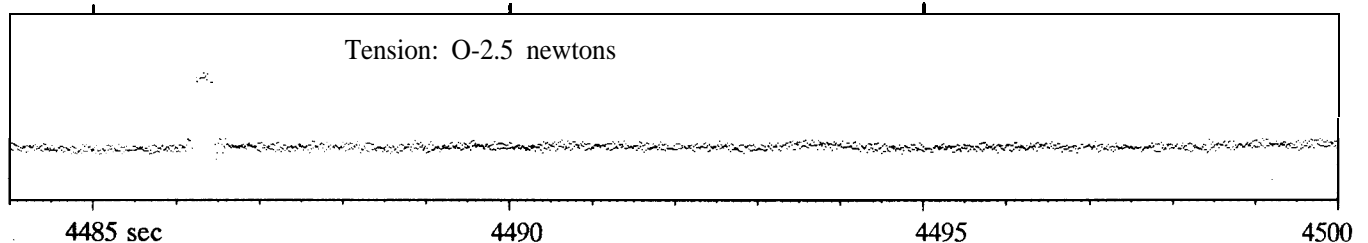


Figure 7. 16-Second High-Speed SEDS-1 Tension Sample, Showing Deployment of First Solder Segment

## Final Notes on SEDS Capabilities

At 4571 seconds, the SEDS computer began to apply active braking, as shown by the bars at the bottom of Figures 5 and 6. The brake ramped tension up to >3 newtons. When the last 100 meters began to deploy, with its embedded solder, the tension doubled again. But tensiometer vibrations caused some readings to be off-scale even though the average may have been on-scale. This resulted in under-estimates of the actual tension. Seconds that included off-scale tension readings are marked at the very bottom of Figure 6. The faster-than-expected deployment and lack of feedback in the brake law caused the end of the tether to be reached at a deployment rate of 7 m/s. This caused a large tether stretch followed by a rebound. Tuning simulations to fit flight data for the rebound indicates a peak tension of order 40 newtons. This is 8 times the peak tension expected with braking to a smooth stop, but still only about 5% of the breaking strength of the tether.

During braking, the tether began to swing down toward the vertical. The mean tension increased during the swing, but due to significant damping in the tether plus energy transfer to other modes, the peak tension during later bounces was lower than that experienced during the first bounce. Data collected by the SEDS-1 payload remained on-scale during these bounces.

The tether cut time was based on a fixed delay of 1040 seconds after the start of active braking. This resulted in payload release near but not at the vertical. This simple logic actually gives lower reentry location dispersions than a more sophisticated logic that tries to cut the tether right at the vertical. Release took place at 5611 seconds, 20 seconds less than one orbit after SEDS powerup.

Since release occurred near apogee and the maximum orbit change is half an orbit later, most of the SEDS orbit change was to perigee. The Delta's perigee was raised several km, and the perigee of the payload and attached tether dropped well into the earth's atmosphere. The payload and tether reentered 1/3 orbit after release. Pre-flight predictions of reentry location were accurate enough that observers stationed in Mexico were able to capture TV imagery of the night-time reentry.

The above discussion of SEDS-1 flight performance can be summarized briefly as follows:

1. Full deployment occurred without problems
2. The data was all received and all made sense
3. Unexpected transverse dynamics caused no problems
4. Pauses in deployment did not induce tether fouling
5. SEDS damped axial tether dynamics very effectively
6. SEDS can be robust against tension estimate errors
7. The brake law needs feedback for controlled stops

Mission-specific SEDS capabilities and constraints are best assessed by using Beadsim, a tether dynamics simulation program for PCs written in Borland Pascal<sup>6</sup>.

Many SEDS applications involve low-tension deployment followed by 3-6 minutes of braking and then a swing to the vertical. The largest deltaV occurs if the payload is deployed at low tension and released in the middle of a wide prograde swing (a forward swing if deploying up, and a backward one if deploying down). This provides 4 m/s of deltaV per km of tether length, a deltaV which is split between payload and host vehicle inversely with their mass. The deltaV is in plane, and has the largest effect on altitude 1/2 orbit after release. Near-vertical stabilization is also possible. It will be tested on SEDS-2, which is now scheduled for March 1994. SEDS-2 braking will start early in deployment and will use rate feedback.

A short tether orbit life minimizes contribution to space debris. In a boost operation, the tether should be cut loose at the vehicle end about 30 minutes after it is cut loose from the payload. This releases the free tether's orbit life during a retrograde libration and can reduce the free tether's orbit life from days to a few hours.

On Delta-based experiments, the Marman clamp limits the deployed payload mass. The existing clamp can hold 25-35 kg, depending on CG offset from the separation plane. The clamp fits between the SEDS deployer and an adjacent electronics bay access door, so envelope constraints may be more severe than mass constraints. Other mounting schemes might relax these constraints. For example, MDAC built a clamp for Losat-X which can handle 60-80 kg, but this clamp mounts centrally between two E-bay access doors. Using it with SEDS requires mounting the SEDS hardware inside the payload. (A smaller SEDS deployer designed for this purpose is now in fabrication.)

SEDS can also boost primary Delta payloads. Since a primary Delta payload weighs much more than the empty 2<sup>nd</sup> stage, such a boost also provides a large deboost to the 2<sup>nd</sup> stage. In cases where slightly negative payload margins exist, SEDS might be used to place a payload in a higher orbit than otherwise feasible, while at the same time deorbiting the 2<sup>nd</sup> stage in a controlled manner.

Economical recovery of reentry capsules requires a small recovery zone. This can be compatible with a wide range of low-speed deployment tensions if that range brackets a cusp value that causes a minimum reentry range. On SEDS-1 the cusp was just over 0.02 newton. The actual SEDS-1 tension was over 50% higher, but that increase did not cause large reentry errors.

## Final Notes on SEDS Capabilities

At 4571 seconds, the SEDS computer began to apply active braking, as shown by the bars at the bottom of Figures 5 and 6. The brake ramped tension up to ~3 newtons. When the last 100 meters began to deploy, with its embedded solder, the tension doubled again. But tensiometer vibrations caused some readings to be off-scale even though the average may have been on-scale. This resulted in under-estimates of the actual tension. Seconds that included off-scale tension readings are marked at the very bottom of Figure 6. The faster-than-expected deployment and lack of feedback in the brake law caused the end of the tether to be reached at a deployment rate of 7 m/s. This caused a large tether stretch followed by a rebound. Tuning simulations to fit flight data for the rebound indicates a peak tension of order 40 newtons. This is 8 times the peak tension expected with braking to a smooth stop, but still only about 5% of the breaking strength of the tether.

During braking, the tether began to swing down toward the vertical. The mean tension increased during the swing, but due to significant damping in the tether plus energy transfer to other modes, the peak tension during later bounces was lower than that experienced during the first bounce. Data collected by the SEDS-1 payload remained on-scale during these bounces.

The tether cut time was based on a fixed delay of 1040 seconds after the start of active braking. This resulted in payload release near but not at the vertical. This simple logic actually gives lower reentry location dispersions than a more sophisticated logic that tries to cut the tether right at the vertical. Release took place at 5611 seconds, 20 seconds less than one orbit after SEDS powerup.

Since release occurred near apogee and the maximum orbit change is half an orbit later, most of the SEDS orbit change was to perigee. The Delta's perigee was raised several km, and the perigee of the payload and attached tether dropped well into the earth's atmosphere. The payload and tether reentered 1/3 orbit after release. Pre-flight predictions of reentry location were accurate enough that observers stationed in Mexico were able to capture TV imagery of the night-time reentry.

The above discussion of SEDS-1 flight performance can be summarized briefly as follows:

1. Full deployment occurred without problems
2. The data was all received and all made sense
3. Unexpected transverse dynamics caused no problems
4. Pauses in deployment did not induce tether fouling
5. SEDS damped axial tether dynamics very effectively
6. SEDS can be robust against tension estimate errors
7. The brake law needs feedback for controlled stops

Mission-specific SEDS capabilities and constraints are best assessed by using Beadsim, a tether dynamics simulation program for PCs written in Borland Pascal<sup>6</sup>.

Many SEDS applications involve low-tension deployment followed by 3-6 minutes of braking and then a swing to the vertical. The largest deltaV occurs if the payload is deployed at low tension and released in the middle of a wide prograde swing (a forward swing if deploying up, and a backward one if deploying down). This provides 4 m/s of deltaV per km of tether length, a deltaV which is split between payload and host vehicle inversely with their mass. The deltaV is in plane, and has the largest effect on altitude 1/2 orbit after release. Near-vertical stabilization is also possible. It will be tested on SEDS-2, which is now scheduled for March 1994. SEDS-2 braking will start early in deployment and will use rate feedback.

A short tether orbit life minimizes contribution to space debris. In a boost operation, the tether should be cut loose at the vehicle end about 30 minutes after it is cut loose from the payload. This releases the free tether's orbit life during a retrograde libration and can reduce the free tether's orbit life from days to a few hours.

On Delta-based experiments, the Marman clamp limits the deployed payload mass. The existing clamp can hold 25-35 kg, depending on CG offset from the separation plane. The clamp fits between the SEDS deployer and an adjacent electronics bay access door, so envelope constraints may be more severe than mass constraints. Other mounting schemes might relax these constraints. For example, MDAC built a clamp for Losat-X which can handle 60-80 kg, but this clamp mounts centrally between two E-bay access doors. Using it with SEDS requires mounting the SEDS hardware inside the payload. (A smaller SEDS deployer designed for this purpose is now in fabrication.)

SEDS can also boost primary Delta payloads. Since a primary Delta payload weighs much more than the empty 2<sup>nd</sup> stage, such a boost also provides a large deboost to the 2<sup>nd</sup> stage. In cases where slightly negative payload margins exist, SEDS might be used to place a payload in a higher orbit than otherwise feasible, while at the same time deorbiting the 2<sup>nd</sup> stage in a controlled manner.

Economical recovery of reentry capsules requires a small recovery zone. This can be compatible with a wide range of low-speed deployment tensions if that range brackets a cusp value that causes a minimum reentry range. On SEDS-1 the cusp was just over 0.02 newton. The actual SEDS-1 tension was over 50% higher, but that increase did not cause large reentry errors.

SEDS can act like a kite tail and stabilize a payload at the beginning of reentry, until the Spectra melts. And even if the payload needs to cut the tether loose before this, an intentional torque imbalance in the tether can provide a several-rpm payload spin about a vertical axis by the time of release. Such vertical-axis spin is suitable for payloads reentering 1/4 to 1/3 orbit later.

Table 1 shows SEDS capabilities with various Spectra tether braid constructions that all have the same mass and volume. The table takes credit for payload orbit changes only. It assumes LEO orbits, a 53° libration angle, a host vehicle with 10 times the payload mass, and a tether safety factor of 4. It also assumes that micrometeoroids with > 1/3 the tether diameter will cut the tether upon impact. Man-made debris increases these risks only slightly. Deployment tests have only been done with 8x375 and 8x215 braids so far, but tests with 4x215 and 24x650 braids are planned in 1994.

Table 1. SEDS Capabilities with Various Tethers

<u>Braid design</u>	<u>Dia mm</u>	<u>MaxL Km</u>	<u>ΔV m/s</u>	<u>MaxPay kg</u>	<u>Impact %/use</u>	<u>Risk DaysLife</u>
24x650	1.7	4.3	15	30,000	0.003	1,000
8x650	1.0	13	46	3,300	0.032	80
8x375	0.75	23	80	1,070	0.11	23
8x215	0.57	40	140	350	0.41	6
4x375	0.53	46	160	270	0.56	4
4x215	0.40	80	280	88	1.9	1

Besides the tether itself, the only changes needed for SEDS to be able to provide a modest boost to even a full shuttle payload of 30,000 kg are the tensiometer and the brake control law. Simulations indicate that control gets easier as the payload mass increases. (The 26 kg SEDS-1 payload was near the minimum feasible.) Standard “two-fault tolerant” rules may require adding redundant sensors and cutters to SEDS, but this appears practical.

### Acknowledgements

SEDS development was funded under SBIR contracts and follow-on contracts with NASA MSFC. George von Tiesenhausen was contract monitor on the first contract, and Jim Harrison has been contract monitor since then. In addition to them, I would like to thank Jim Arnold, Ivan Bekey, George Levin, Chris Rupp, Sid Saucier, and J.R. Thompson for their support, and my colleagues Chuck Alexander, Mike Carpenter, Jim Clinton, Kevin Cross, Mike Fennell, George Henschke, Marianne Knight, Matt Nilsen, John Oldson and Eric Pulliam for all of their work on SEDS.

### References

1. SEDS: The Small Expendable-tether Deployment System, Final Report on NASA SBIR Phase II Contract NAS8-35256, Energy Science Laboratories, Inc., December 1987. Available from NASA Marshall.
2. Final Report on SEDS Experiment Design Definition Contract NAS8-37380, Energy Science Laboratories, Inc., February 1990. Available from NASA Marshall.
3. Space Systems Division CLM/CLFP/CWN Policy for Secondary Payloads on Delta II, August 1989. Available from CLMD, USAF HQ Space Division, Los Angeles AFB, CA 90009-2960.
4. L. Melfi, Jr., Engineering Performance of the SEDS-1 End Mass Payload, AIAA paper 93-4769, Space Programs and Technologies Conference, Huntsville, September 1993.
5. John Glaese, Comparison of SEDS-1 Pre-Flight Simulation and Flight Data, AIAA paper 93-4766, Space Programs and Technologies Conference, Huntsville, September 1993.
6. Beadsim: Beadsim is an easy-to-use tether dynamics simulation program for PCs, written in Borland Pascal 7.0. Available from NASA Marshall or Tether Applications on a floppy disk containing source and executable code, sample cases, and a help file.

### Bibliography

- Delta II Commercial Spacecraft Users Manual, MDC H3224A, McDonnell Douglas, July 1989.
- Delta II Secondary User’s Guide, available from NASA Goddard, Huntington Beach (at McDonnell Douglas).
- NASA Tethers in Space Handbook, Second Edition, prepared by SRS Technologies for NASA Headquarters, Code MD, May 1989. Overview of tether applications and tether dynamics, with extensive bibliography.